Structure
Short Article

Crystal Structure of the Homology Domain of the Eukaryotic DNA Replication Proteins Sld3/Treslin

Hiroshi Itou,[1,3,*] Sachiko Muramatsu,[2] Yasuo Shirakihara,[1,3] and Hiroyuki Araki[2,3,*]
[1]Structural Biology Center, National Institute of Genetics, Yata1111, Mishima, Shizuoka 411-8540, Japan
[2]Division of Microbial Genetics, National Institute of Genetics, Yata1111, Mishima, Shizuoka 411-8540, Japan
[3]Department of Genetics, SOKENDAI, Yata1111, Mishima, Shizuoka 411-8540, Japan
*Correspondence: hitou@nig.ac.jp (H.I.), hiaraki@nig.ac.jp (H.A.)
http://dx.doi.org/10.1016/j.str.2014.07.001

SUMMARY

The initiation of eukaryotic chromosomal DNA replication requires the formation of an active replicative helicase at the replication origins of chromosomal DNA. Yeast Sld3 and its metazoan counterpart Treslin are the hub proteins mediating protein associations critical for the helicase formation. Here, we show the crystal structure of the central domain of Sld3 that is conserved in Sld3/Treslin family of proteins. The domain consists of two segments with 12 helices and is sufficient to bind to Cdc45, the essential helicase component. The structure model of the Sld3-Cdc45 complex, which is crucial for the formation of the active helicase, is proposed.

INTRODUCTION

Chromosomal DNA replication is tightly regulated in eukaryotic cells such that each replication origin in DNA fires just once at the correct time during the cell cycle. The activation of the replicative helicase, which unwinds the double-stranded DNA, permitting DNA polymerase to synthesize DNA, is a key step of the regulation. Active helicase is formed by loading of two essential components, Cdc45 and GINS, onto the Mcm2-7 helicase core complex on the replication origin (Moyer et al., 2006). This process requires another set of replication proteins, and in budding yeast, one of the essential replication proteins, Sld3, has emerged as a focal point of regulation in origin firing. Sld3 and Cdc45 form a complex that associates with origins in a mutually dependent manner (Kamimura et al., 2001). The recruitment of Sld3 to origins depends on the phosphorylation of the helicase core complex by Dbf4-dependent kinase (DDK) (Masai et al., 2006; Sheu and Stillman, 2006, 2010). On the other hand, Sld3 is a substrate of cyclin-dependent kinase (CDK) (Tanaka et al., 2007; Zegerman and Diffley, 2007), and the further phosphorylation of Sld3 by a CDK recruits GINS to origins by interacting with Dpb11 (Muramatsu et al., 2010), resulting in the formation of a transient intermediate, preinitiation complex. Sld3 is well conserved in yeast and fungi, and its functional counterpart Treslin (also known as Ticrr) was found in metazoan (Kumagai et al., 2010; Sansam et al., 2010). Sld3 and Treslin differ in their molecular sizes and amino acid sequences, except in the limited region called the Sld3/Treslin domain (Sanchez-Pulido et al., 2010), suggesting that this domain is important for their common function; however, the role of the conserved Sld3/Treslin domain remains elusive because of a lack of structural and biochemical information.

In this study, we elucidated the structural basis for the function of the Sld3/Treslin domain. We determined the crystal structure of the domain of budding yeast Sld3, and our structural and functional analyses showed that the domain is a rhombic-shaped molecule, consists of 2 segments with 12 helices, and is sufficient to bind to Cdc45. The properties of the Cdc45-binding site of the Sld3/Treslin domain seems to be complementary to that of the proposed model of Cdc45. Based on the results, we discuss the structure model of the Sld3-Cdc45 complex.

RESULTS AND DISCUSSION

The Sld3/Treslin Domain Comprising the Cdc45-Binding Domain

Genetic evidence suggests that the Sld3/Treslin domain interacts with Cdc45 (Kamimura et al., 2001; Nakajima and Masukata, 2002; Tanaka et al., 2011b). To test the physical interaction between the Sld3/Treslin domain of Sld3 (Ser148-Lys430; Figure 1A) and Cdc45 of budding yeast, both proteins were coexpressed in *Escherichia coli* cells and examined to determine whether they could be copurified. A His tag was connected to the domain, allowing the protein to be purified from the cell extract using Ni-affinity resin. The result showed that Cdc45 did copurify with the Sld3/Treslin domain (Figures 2A and 2B). The intensity of the protein bands showed that these proteins bind in a stoichiometric one-to-one ratio (Figure 2A), indicating the domain alone is sufficient to form a stable complex with Cdc45. Therefore, we named the Sld3/Treslin domain the *C*dc45-*b*inding *d*omain (Sld3-CBD).

The Properties of Sld3-CBD Seem to Be Complementary to the Supposed Structure Model of Cdc45

Sld3-CBD (Ser148-Lys430) was crystallized, and its tertiary structure was determined (Table 1). This domain shows a rhombic-shaped compact structure with 12 helices (Figure 1B). Helix H7 passes through the center of the molecule as a backbone, and the other helices are placed around the helix through hydrophobic interactions.

Sld3-CBD does not perfectly match the Sld3/Treslin domain proposed by the bioinfomatic study (Sanchez-Pulido et al.,

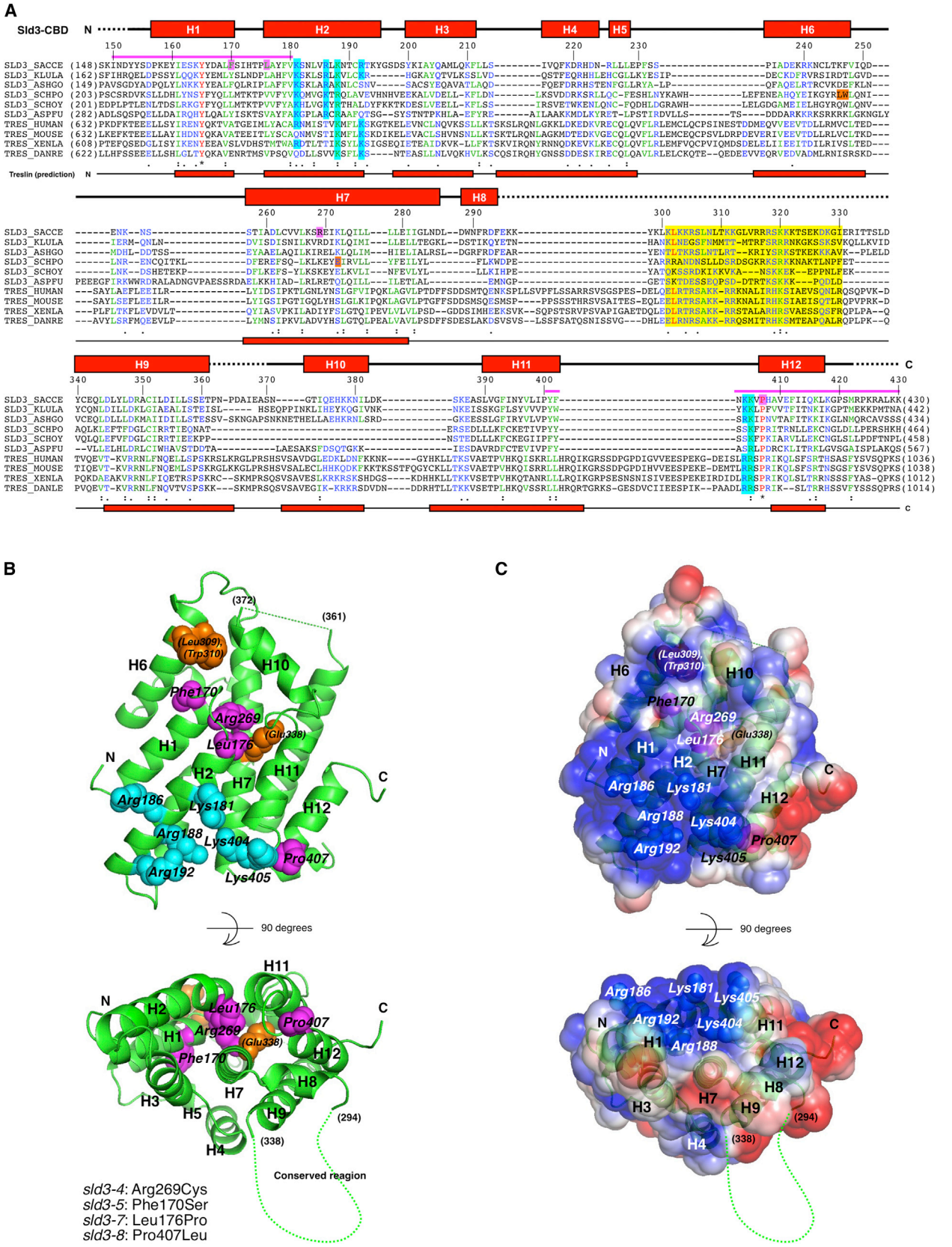

(legend on next page)

2010); it comprises an extra N-terminal region. This extended part contains one of the regions necessary to interact with Cdc45 (Tanaka et al., 2011b), and the amino acid sequences in this region also showed homology among the Sld3/Treslin proteins (Figure 1A). The crystal structure of Sld3-CBD clearly showed that both of the regions necessary to bind to Cdc45 (Tanaka et al., 2011b) belong to the same structural domain; furthermore, these two regions are on the same side of the molecule (helices H1–H2 and H11–H12: Figures 1A and 1B). More interesting, amino acid substitutions of Sld3-CBD that weaken the interaction with Cdc45 (Kamimura et al., 2001) (Figure 1A) were mapped on the same surface, suggesting that this side of Sld3-CBD interacts with Cdc45 (Figure 1B).

The compact structure of Sld3-CBD seems to fit well with its binding partner, Cdc45. Small-angle X-ray scattering (SAXS) suggested that Cdc45 is a V-shaped molecule comprising a core region with lateral extensions (Krastanova et al., 2012; Szambowska et al., 2014). In addition, bioinformatic analyses revealed a homology between Cdc45 and RecJ, which belongs to the DHH family (Krastanova et al., 2012; Sanchez-Pulido and Ponting, 2011). Structural superimposition and sequence alignment of the proteins suggested that the characteristic acidic insertion occurred on the concave surface of the core region of Cdc45 (Krastanova et al., 2012).

The Conserved Acidic Region of Cdc45 Is Important for the Interaction with Sld3

We then tested the function of the acidic region of Cdc45 for Sld3 binding. The homology model of the DHH homology domain of human Cdc45 (Sanchez-Pulido and Ponting, 2011) suggested that the amino acids substituted in the *cdc45* mutation *cdc45-27* (Leu131-Pro) (Kamimura et al., 2001), which weaken the interaction between Sld3 and Cdc45, are on the concave surface of the Cdc45. Thus, we substituted the conserved acidic residues near the mutation site. The Cdc45 D2N mutant, whose Asp91, Asp124, Asp149, and Asp150 were substituted with Asn, was coexpressed with the His-tagged Sld3-CBD in *E. coli* cells, and the Sld3-CBD was purified from the cell extract. The result showed that Cdc45 D2N significantly reduced its binding capacity to Sld3-CBD (Figure 2B). This result is consistent with phenotype of *cdc45* D2N cells, which grow very slowly at 34°C and whose growth was restored by high-copy *SLD3* (Figure 2C). Phenotypic defects caused by reduced protein interaction are often restored by an increased dosage of the partner protein. These results indicated that the conserved acidic region, which is supposed to be located on the concave surface of Cdc45, is important to the interaction with Sld3.

The Conserved Flexible Region in Sld3-CBD Is Responsible for the Formation of the Complex with Cdc45

The crystal structure showed that Sld3-CBD has two conserved basic regions as the possible binding site for the conserved acidic region of Cdc45. One is the region from residue 301–330 of Sld3. This region is conserved in Sld3/Treslin proteins and comprises many basic residues, although the region seems to be structurally flexible (Figures 1A and 1B). We hypothesized that this flexible region functions to bind to Cdc45. To test this hypothesis, we coexpressed the His-tagged Sld3-CBD (Δ301–330) lacking the conserved 30 amino acids of this region and Cdc45 in *E. coli* cells, and purified the Sld3-CBD using Ni-affinity resin. The deletion of the 30 amino acids significantly reduced the recovery of Cdc45 (Figure 2B), indicating a reduced binding capacity of Sld3-CBD (Δ301–330) to Cdc45. This is consistent with phenotype of *sld3* Δ301–330 cells, which grow very slowly at 37°C and whose growth was restored by high-copy *CDC45* (Figure 2D). Moreover, direct interaction between the peptide consituting the conserved flexible region (residue numbers 296–332) and Cdc45 was observed in in vitro analysis. Cdc45 protein could be copurified with the His-tagged Sld3 peptide using Ni-affinity resin (Figure 3). The result also showed that

Figure 1. Amino Acid Sequence Alignment and the Crystal Structure of the Homology Domain Shared by Sld3/Treslin Family Proteins

(A) Alignment of the Sld3/Treslin domain from fungal Sld3 (SACCE: *S. cerevisiae;* KLULA: *Kluyveromyces lactis*; ASHGO: *Ashbya gossypii*; SCHPO: *Schizosaccharomyces pombe;* SCHOY: *Schizosaccharomyces octosporus;* ASPFU: *Aspergillus fumigatus*) and Treslin/Ticrr from vertebrates (HUMAN: *Homo sapiens;* MOUSE: *Mus musculus;* DANRE: *Danio rerio*;and XENLA: *Xenopus laevis*) is shown. Hyphens indicate deletions. CLUSTAL W (Larkin et al., 2007) was used to create the initial alignment, and it was further aligned to match the secondary structures of Sld3/Treslin proteins predicted using the Phyre2 structure prediction server (Kelley and Sternberg, 2009) to that of Sld3-CBD determined by the crystal structure. The secondary structure of human Treslin predicted by the server and that of Sld3-CBD determined by the crystal structure in this study are indicated below and above the alignment, respectively. Dashed lines in the secondary structure of Sld3-CBD indicate disordered regions in the crystal. The conserved (*) and the conserved change (: and .) amino acids are marked below the alignment and also colored in red, green, and blue. The numbers in parentheses beside the sequences indicate residue numbers of each protein, and the residue numbers of *S. cerevisiae* Sld3 is indicated above the alignment. The conserved region found in the structurally disordered region (residue numbers 301–330 in *S. cerevisiae* Sld3) is highlighted with a yellow box. Positions of the amino acid substitutions in the mutations that showed temperature-sensitive (TS) growth identified from *S. cerevisiae* (*sld3-4*: Arg269Cys+ Asp578Gly; *sld3-5*: Gly125Asp+ Phe170Ser; *sld3-7*: Leu176Pro; and *sld3-8*: Pro407Leu) (Kamimura et al., 2001) are highlighted with magenta boxes, and those from *S. pombe* (*Sp sld3-10*: Glu338Gly; *Sp sld3-41*: Ser153Leu+ Leu309Pro; and *Sp sld3-52*: Trp310Arg) (Nakajima and Masukata, 2002) are highlighted with orange boxes. The regions necessary for binding with Cdc45, suggested by yeast two-hybrid analysis (Tanaka et al., 2011b), are shown with magenta lines above the alignment. The basic residues conserved near the presumed Cdc45-binding interface and forming the positively charged region are highlighted with sky-blue boxes.

(B) Ribbon representations of the crystal structure of Sld3-CBD. The atomic model from Tyr154 to Ser421 was obtained. The structure for the regions Glu295-Asp337 and Pro362-Asn371 could not be placed because of poor electron density caused by structural disorder. The crystallographic asymmetric unit contained three Sld3-CBD molecules. Views of the molecule are from the direction perpendicular (top panel) and coaxial (bottom panel) to the backbone helix H7. The top panel shows the presumed Cdc45-binding interface suggested by genetic analyses (Kamimura et al., 2001; Tanaka et al., 2011b). The amino acids substituted in the TS mutants *sld3-4*, *sld3-5*, *sld3-7*, and *sld3-8* (Kamimura et al., 2001) and in *Sp sld3-10*, *Sp sld3-41*, and *Sp sld3-52* (Nakajima and Masukata, 2002) and the conserved basic amino acids forming the basic patch are shown in magenta, orange, and sky blue, respectively, in the space-filling model. The representations of the protein tertiary structure in this figure were generated using PyMOL (Schrödinger).

(C) Surface-charge representation of Sld3-CBD. The direction of view is the same as in (B). The surface electric potential was calculated using APBS (Baker et al., 2001). Blue and red on the molecular surface show the positively and negatively charged regions, respectively.

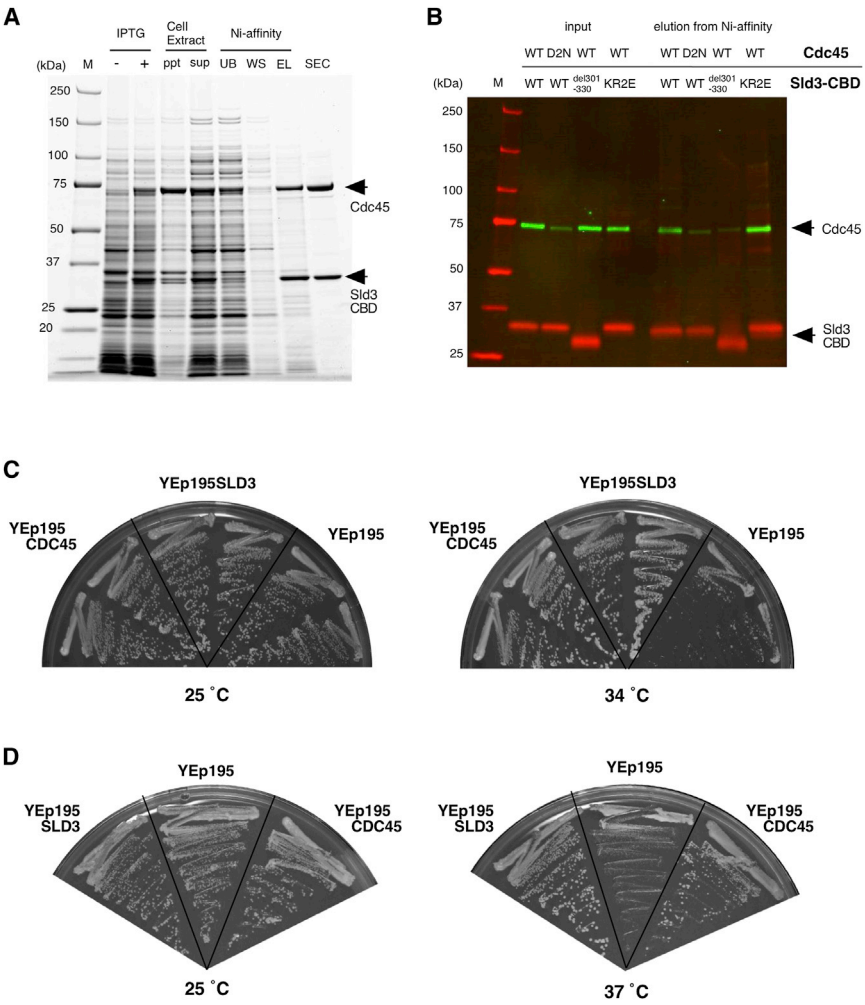

Figure 2. Analyses of the Interaction between Sld3 and Cdc45

(A) Sld3-CBD (Ser148-Lys430, molecular mass 33.1 kDa) and the full-length Cdc45 (molecular mass 74.2 kDa) were coexpressed in *E. coli*. Sld3-CBD was purified using a His tag connected to it. The lanes are labeled as follows, M, molecular weight markers; ppt, insoluble fraction from the cell extract; sup, lysate of the cell extract; UB, unbound fraction from Ni-affinity chromatography; WS, fraction washed from the Ni-affinity resin;, EL, eluate from the Ni-affinity resin. In this analysis, the eluted fraction (lane EL) was further purified using size-exclusion chromatography (SEC) to remove free Sld3-CBD (Figure S2).

(B) The lysate of the cell extract (input) and the eluate from the Ni-affinity resin were analyzed using immunoblotting using anti-Sld3 (red) and anti-Cdc45 (green) antibodies (Tanaka et al., 2011a). The interaction between the mutated Sld3-CBD and Cdc45 was also analyzed in vitro using the purified proteins (Figure S3).

(C) The plasmids YEp195CDC45 (high-copy plasmid expressing Cdc45; positive control), YEp195 (vector only; negative control), and YEp195SLD3 (high-copy plasmid expressing Sld3) were transformed into *cdc45Δ::LEU2* bearing YCp22*cdc45* (D2N) and incubated at the indicated temperature for 3 days.

(D) The plasmids YEp195SLD3 (high-copy plasmid expressing Sld3; positive control), YEp195 (vector only; negative control), and YEp195CDC45 (high-copy plasmid expressing Cdc45) were transformed into *sld3Δ::LEU2* bearing YCp22*sld3* (Δ301–330) and incubated at the indicated temperature for 2 days.

the binding capacities of Sld3-CBD and the peptide to Cdc45 D2N protein are significantly reduced (Figure 3).

Another candidate that could be responsible for the binding to the acidic region of Cdc45 was found near the presumed Cdc45-binding interface suggested by the genetic analyses (Kamimura et al., 2001; Tanaka et al., 2011b) (Figure 1C). The basic residues clustered in the region are well conserved among the Sld3/Treslin proteins (Figure 1A). To test function of the basic region for the interaction with Cdc45, the basic amino acids clustered here were mutated (Sld3-CBD KR2E mutant). In this mutant, the basic amino acids conserved among the Sld3/Treslin proteins and their side chain are directed toward the solvent area in the crystal structure of Sld3-CBD, whose Lys181, Arg186, Arg192, Lys404, and Lys405 were substituted with Glu. The His-tagged Sld3-CBD KR2E protein was coexpressed with Cdc45 in *E. coli* cells, and the Sld3-CBD mutant was purified using Ni-affinity resin. The result showed that the mutations did not show an obvious effect on the binding capacity of Sld3-CBD to Cdc45 (Figure 2B). However, the Sld3 KR2E mutation did cause a severe phenotypic defect in yeast; the *sld3* KR2E cells were not viable (Figure S1 available online). These results indicated that the conserved basic region of Sld3-CBD is important for functions other than Cdc45 binding.

The Model of the Sld3-Cdc45 Complex and Its Functional Significance

These results allowed us to consider the binding model of Sld3 and Cdc45 (Figure 4). The convex-shaped compact structure of Sld3-CBD seems to fit with that of its binding partner Cdc45, suggested in the previous studies (Krastanova et al., 2012; Szambowska et al., 2014). The conserved acidic region of Cdc45, which is supposed to be located on the concave surface of the molecule, is important for the interaction with Sld3. Interaction between the acidic region and the conserved basic region of Sld3 (residue numbers 301–330) is important for complex formation. The conserved basic region of Sld3 is structurally flexible, and this flexibility may be important for the formation of a stable complex. Another binding interface for Cdc45 that was suggested by the previous genetic analyses (Kamimura et al., 2001; Tanaka et al., 2011b) is located on the convex surface of Sld3-CBD. Amino acid substitutions that weaken the interaction with Cdc45 (Kamimura et al., 2001) are mapped onto the loop regions connecting the helices on the binding interface and on helix H7 near the loops (Figure 1B), suggesting that the shape of the interface is important to maintain the interaction with Cdc45. Although the tertiary structure of fission yeast Sld3 is not available, the amino acid alignment of the Sld3/Treslin

Table 1. Summary of Data Collection and Refinement Statistics

Data Collection (Beamline PF-NE3A)		
Parameters	Native	Se-SAD (Peak)
Wavelength (Å)	1.00000	0.97889
Resolution (Å)[a]	50.0 – 2.40 (2.44 – 2.40)	50.0 – 2.80 (2.85 – 2.80)
Cell bonds (Å)	a = 65.3, b = 92.8, c = 160.9	a = 66.2, b = 92.5, c = 160.7
Cell angles (°)	$\alpha = \beta = \gamma$ = 90.0	$\alpha = \beta = \gamma$ = 90.0
Space group	$P2_12_12_1$	
Unique reflections	39,283	25,250
Completeness (%)	99.2 (98.0)	99.6 (100)
Averaged redundancy	10.8 (9.5)	10.8 (10.7)
Mean I/σ	34.6 (3.7)	32.8 (5.4)
R_{merge} (%)[b]	6.5 (40.0)	7.3 (47.8)
Refinement		
Resolution range of data used (Å)	19.6–2.4	
Reflections used	32,583	
R factor (%)[c]	21.7	
Free R factor (%)[d]	26.2	
Average B factor (Å^2)	48.93	
Number of protein molecules in asymmetric unit	3	
Total number of nonhydrogen atoms		
Protein	5,193	
Nonprotein	111	
Solvent	178	
Rmsd from standard values		
Bonds (Å)	0.018	
Angles (°)	2.008	
Ramachandran plot[e]		
Residues in favored regions (%)	97.9	
Residues in allowed region (%)	2.0	
Residues in disallowed region (%)	0.1	

[a]Values in parentheses are for the outermost resolution shell.
[b]$R_{merge} = \sum_h\sum_j |\langle I\rangle_h - I_{h,j}| / \sum_h\sum_j I_{h,j}$ where $\langle I\rangle_h$ is the mean intensity of symmetry-equivalent reflections.
[c]R factor = $\sum|F_{obs} - F_{cal}|/\sum F_{obs}$, where F_{obs} and F_{cal} are the observed and calculated structure factor amplitudes, respectively.
[d]Free R factor value was calculated for R factor using only an unrefined subset of reflections data (5%).
[e]Ramachandran plot was calculated using RAMPAGE (Lovell et al., 2003).

proteins suggests that the mutations in Sld3 that weaken the interaction with Cdc45 in fission yeast (Nakajima and Masukata, 2002) are also located on the same convex surface (Figures 1A and 1B). Because Cdc45 is twice as large as Sld3-CBD and is thought to be a V-shaped molecule comprising lateral extensions, this molecule can bind to both Cdc45-binding segments of Sld3, although the two segments lie on opposite sides of the molecule.

Such extensive interactions between Sld3 and Cdc45 through two spatially separated segments may induce conformational changes in Cdc45 for loading onto the Mcm2-7 complex. This

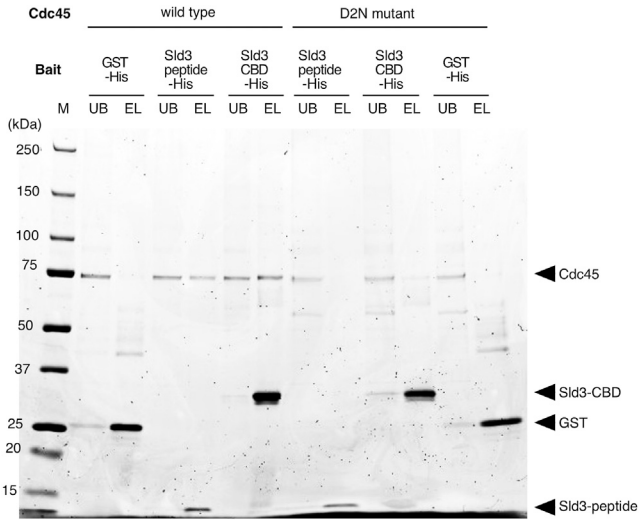

Figure 3. Analysis of the Interaction between Cdc45 and the Conserved Structurally Flexible Region of Sld3-CBD
The purified Cdc45 protein was mixed with various His-tagged versions of GST (negative control), Sld3-CBD (positive control), and Sld3 peptide (residues 296–332), and the His-tagged proteins were collected using Ni-affinity resin. The lanes are labeled as follows: M, molecular weight marker; UB, unbound fraction from the Ni-affinity resin; EL, eluate from the Ni-affinity resin.

is because Cdc45 is not loaded onto the Mcm proteins properly without Sld3/Treslin (Heller et al., 2011; Kamimura et al., 2001; Kumagai et al., 2010; Nakajima and Masukata, 2002). It is possible that these Sld3/Treslins work as molecular chaperones, forming a complex that changes or stabilizes the conformation of Cdc45 to make it suitable for binding to the Mcm proteins. The structure of free Cdc45 estimated by the SAXS analyses (Krastanova et al., 2012; Szambowska et al., 2014) does not fully match that of Cdc45 in the active replicative helicase complex, as analyzed by cryoelectron microscopy (Costa et al., 2011); free Cdc45 has a rather elongated conformation, suggesting a conformational change of the protein, which supports the hypothesis.

The conserved basic region observed near the Cdc45-binding interface on the convex surface of Sld3-CBD did not directly contribute to the interaction with Cdc45. However, this region is indispensable for cell viability, indicating its functional importance for functions other than Cdc45 binding. Because the basic residues clustered in this region are highly conserved among the Sld3/Treslin proteins, it is possible that the region is the binding interface for the other conserved replication proteins. Sld3 seems to bind to the DDK-phosphorylated Mcm proteins (Heller et al., 2011; Tanaka et al., 2011a; Yabuuchi et al., 2006); therefore, their binding interface is expected to have a positive charge. At present, we cannot rule out the possibility that the formation of the Sld3-Cdc45 complex creates the binding interface for the Mcm proteins; the conserved basic region is a potential binding site for phosphorylated Mcm to form a preinitiation complex.

EXPERIMENTAL PROCEDURES

Coexpression of Cdc45 and the Sld3/Treslin Domain of Yeast Sld3

The Sld3/Treslin domain of Sld3 (Sld3-CBD, residue numbers 148–430) and the full-length Cdc45 of *Saccharomyces cerevisiae* were coexpressed in

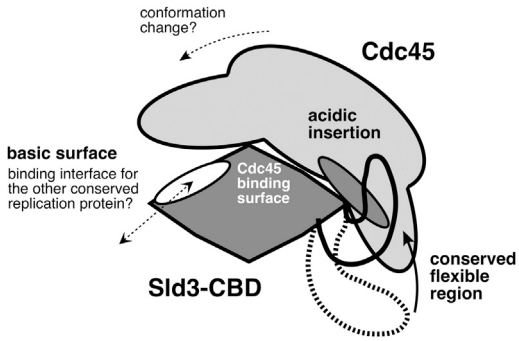

Figure 4. The Model of Sld3-Cdc45 Complex

Our results suggest that Sld3-CBD is sufficient for binding with Cdc45. Sld3-CBD has two binding segments for the interaction: the conserved structurally flexible region and the convex surface suggested by genetic analyses (Kamimura et al., 2001; Tanaka et al., 2011b). The former is indicated to interact with the acidic concave surface of the Cdc45 core region, and the latter is expected to interact with the lateral extension of Cdc45. These extensive interactions through two spatially separated segments may induce conformational changes in Cdc45 to enable it to bind to the Mcm2-7 complex.

E. coli using a pET-Duet1 tandem expression vector (Merck Millipore, Darmstadt). To connect a His tag to the C terminus of the Sld3/Treslin domain, an extra 24 nucleotides encoding an octapeptide comprising hexahistidines (LEHHHHHH) was added to the 3′ end of the domain of Sld3 gene. The protein was purified using the Ni-affinity column (His-spintrap; GE Healthcare Life Sciences) equilibrated with a buffer containing 20 mM Tris-HCl (pH 7.5), 0.3 M NaCl, 20 mM imidazole, and 10% glycerol, and the bound proteins were eluted with a buffer containing 20 mM Tris-HCl (pH 7.5), 0.3 M NaCl, 0.5 M imidazole, and 10% glycerol. The fractions were analyzed using SDS-PAGE. After western blotting, the proteins were visualized and quantified using fluorescence-conjugated secondary antibodies and the Odyssey infrared imaging system (LI-COR Biosciences).

The same experiments were performed with the combinations of the mutant Sld3-CBD (Δ301–330, the Sld3-CBD lacking the residues from position 301 to 330; and KR2E, the Sld3-CBD containing Lys181Glu, Arg186Glu, Arg192Glu, Lys404Glu, and Lys405Glu substitutions) and Cdc45, and of Sld3-CBD and the mutant Cdc45 (D2N, the Cdc45 containing Asp91Asn, Asp124Asn, Asp149Asn, and Asp150Asn substitutions).

Preparation and Crystallization of Sld3-CBD Protein

The His-tagged Sld3-CBD protein was expressed in *E. coli* using the pET-26b (+) vector (Merck Millipore). The protein was purified using the His-trap crude FF column (GE Healthcare Life Science) equilibrated with a buffer containing 20 mM Tris-HCl (pH 7.5), 0.3 M NaCl, 20 mM imidazole, and 10% glycerol. The bound proteins were eluted with a buffer containing 20 mM Tris-HCl (pH 7.5), 0.3 M NaCl, 0.5 M imidazole, and 10% glycerol. The eluate was applied to a Resource S column (GE Healthcare Life Sciences) equilibrated with a buffer containing 20 mM piperazine-N,N′-bis(2-ethanesulfonic acid (PIPES)-NaOH (pH 6.6) and 0.2 M NaCl, and the bound proteins were eluted using a linear gradient of NaCl from 0.2 to 1.0 M in 20 mM PIPES-NaOH (pH 6.6). The Sld3-containing fraction was further purified using a Superdex 200pg column (GE Healthcare Life Sciences) equilibrated with a buffer containing 20 mM Tris-HCl (pH 7.5), 0.3 M NaCl, and 10% glycerol. The purified protein was dialyzed against a buffer containing 10 mM Tris-HCl (pH 7.5), 0.2 M NaCl, and 1 mM dithiothreitol (DTT) and concentrated to 33 mg/ml using an ultrafiltration device (Vivaspin, Sartorius Stedim Biotech, Goettingen) prior to crystallization. Crystallization experiments were performed using the vapor-diffusion method, and the best crystals were obtained under conditions consisting of 0.1 M Tris-HCl (pH 8.4), 0.1 M lithium sulfate, and 12.5% polyethylene glycol 4000 (PEG 4K) at 20°C. The selenomethionine (Se-Met)-substituted Sld3-CBD for single-wavelength anomalous diffraction (SAD) analysis was purified similarly; the growth medium was changed from Luria-Bertani (LB) to the M9 medium supplemented with 25 μg/ml Se-Met. The Se-Met-substituted Sld3-CBD was crystallized under conditions consisting of 0.1 M Tris-HCl (pH 8.0), 0.1 M lithium sulfate, and 10% PEG 4K.

Data Collection and Structure Determination

X-ray diffraction data were collected from the cryocooled crystals (supplemented with 20% [v/v] ethylene glycol as a cryoprotectant) on the structural biology Beamline BL-NE3A in the Photon Factory (KEK, Tsukuba). The native and SAD data were collected at wavelengths 1.00000 and 0.97889 Å, respectively, and processed using HKL2000 (Otwinowski and Minor, 1997). The structure was determined using the SAD method using SOLVE (Terwilliger and Berendzen, 1999) and PHASER (McCoy et al., 2007) in PHENIX suite (Adams et al., 2010). The initial atomic model was obtained using RESOLVE (Terwilliger, 2000, 2003), and the remaining parts were built manually using COOT (Emsley and Cowtan, 2004). The model was refined using the native data up to 2.4 Å resolution using LAFIRE (Yao et al., 2006) with REFMAC5 (Murshudov et al., 1997) in CCP4 suite (CCP4, 1994). The data collection, phasing, and model refinement are summarized in Table 1.

In Vivo Analyses of the Sld3 and Cdc45 Mutants

Plasmid YEp195CDC45 of YS4 cells (Δ*cdc45::LEU2* [YEp195CDC45]) (Tak, 2004) was replaced with YCp22CDC45 (D2N) using the plasmid-shuffling method (Kamimura et al., 2001). The resulting cells were used for the transformation of various plasmids. The transformants were streaked onto SD-Trp, Leu, Ura plates and incubated at 25°C and 34°C for 3 days. Plasmid YEp195SLD3 of YYK13 cells (Δ*sld3::LEU2* [YEp195SLD3]) (Kamimura et al., 2001) was replaced with YCp22SLD3 (Δ301–330), and the resultant cells were used for the subsequent transformation of various plasmids. The transformants were streaked onto SD-Trp, Leu, Ura plates and incubated at 25°C and 37°C for 2 days.

Construction of the Plasmids Expressing the Mutated Proteins

All the plasmids expressing the mutated proteins used in this study were prepared using PCR using the PrimeSTAR Mutagenesis kit (Takara Bio, Shiga).

In Vitro Binding Assay

His-tagged Sld3 peptide (residue numbers 269–332) and glutathione S-transferase (GST) were expressed in *E. coli* using pET26b (+) vector (Merck Millipore) and purified using the Ni-affinity column (His-trap crude FF). Flag-tagged Cdc45 and Cdc45 D2N proteins were respectively expressed in *E. coli* and purified using M2 agarose beads (Sigma-Aldrich). The purified proteins were dialyzed against a buffer containing 20 mM Tris-HCl (pH 7.5), 0.3 M NaCl, 0.005% Triton X-100, and 10% glycerol. Four micromoles of the His-tagged Sld3-CBD, Sld3 peptide, and GST were each mixed with 0.4 μM of the purified Cdc45 or Cdc45 D2N and incubated for 0.5 hr on ice. The mixtures were applied to the Ni-affinity column (His-spintrap) equilibrated with the dialysis buffer, and the His-tagged proteins were eluted using a buffer containing 20 mM Tris-HCl (pH 7.5), 0.3 M NaCl, 0.5 M imidazole, 0.005% Triton X-100, and 10% glycerol. The fractions were analyzed using SDS-PAGE.

ACCESSION NUMBERS

Coordinate and structure factors for the crystal structure have been deposited in Protein Data Bank under the accession code 3WI3.

SUPPLEMENTAL INFORMATION

Supplemental Information includes three figures and can be found with this article online at http://dx.doi.org/10.1016/j.str.2014.07.001.

AUTHOR CONTRIBUTIONS

H.I. designed and performed all the experiments, except the yeast genetics, and wrote the paper. S.M. performed the yeast genetics. Y.S. helped with the discussion. H.A. supervised the project and wrote the paper.

ACKNOWLEDGMENTS

We thank the staff of Beamline BL-NE3A, KEK for their help with diffraction data collection. This work was supported by a Grant-in-Aid for Scientific Research on Innovative Areas (Structural cell biology, grant number 25121736 to H.I.), and a Grant-in-aid for Scientific Research (A) (grant number 25251005 to H.A.) from the Ministry of Education, Culture, Sports, Science and Technology, Japan (MEXT).

Received: December 2, 2013
Revised: June 5, 2014
Accepted: July 3, 2014
Published: August 7, 2014

REFERENCES

Adams, P.D., Afonine, P.V., Bunkóczi, G., Chen, V.B., Davis, I.W., Echols, N., Headd, J.J., Hung, L.W., Kapral, G.J., Grosse-Kunstleve, R.W., et al. (2010). PHENIX: a comprehensive Python-based system for macromolecular structure solution. Acta Crystallogr. D Biol. Crystallogr. *66*, 213–221.

Baker, N.A., Sept, D., Joseph, S., Holst, M.J., and McCammon, J.A. (2001). Electrostatics of nanosystems: application to microtubules and the ribosome. Proc. Natl. Acad. Sci. USA *98*, 10037–10041.

CCP4 (Collaborative Computational Project, Number 4) (1994). The CCP4 suite: programs for protein crystallography. Acta Crystallogr. D Biol. Crystallogr. *50*, 760–763.

Costa, A., Ilves, I., Tamberg, N., Petojevic, T., Nogales, E., Botchan, M.R., and Berger, J.M. (2011). The structural basis for MCM2-7 helicase activation by GINS and Cdc45. Nat. Struct. Mol. Biol. *18*, 471–477.

Emsley, P., and Cowtan, K. (2004). Coot: model-building tools for molecular graphics. Acta Crystallogr. D Biol. Crystallogr. *60*, 2126–2132.

Heller, R.C., Kang, S., Lam, W.M., Chen, S., Chan, C.S., and Bell, S.P. (2011). Eukaryotic origin-dependent DNA replication in vitro reveals sequential action of DDK and S-CDK kinases. Cell *146*, 80–91.

Kamimura, Y., Tak, Y.S., Sugino, A., and Araki, H. (2001). Sld3, which interacts with Cdc45 (Sld4), functions for chromosomal DNA replication in Saccharomyces cerevisiae. EMBO J. *20*, 2097–2107.

Kelley, L.A., and Sternberg, M.J. (2009). Protein structure prediction on the Web: a case study using the Phyre server. Nat. Protoc. *4*, 363–371.

Krastanova, I., Sannino, V., Amenitsch, H., Gileadi, O., Pisani, F.M., and Onesti, S. (2012). Structural and functional insights into the DNA replication factor Cdc45 reveal an evolutionary relationship to the DHH family of phosphoesterases. J. Biol. Chem. *287*, 4121–4128.

Kumagai, A., Shevchenko, A., Shevchenko, A., and Dunphy, W.G. (2010). Treslin collaborates with TopBP1 in triggering the initiation of DNA replication. Cell *140*, 349–359.

Larkin, M.A., Blackshields, G., Brown, N.P., Chenna, R., McGettigan, P.A., McWilliam, H., Valentin, F., Wallace, I.M., Wilm, A., Lopez, R., et al. (2007). Clustal W and Clustal X version 2.0. Bioinformatics *23*, 2947–2948.

Lovell, S.C., Davis, I.W., Arendall, W.B., 3rd, de Bakker, P.I., Word, J.M., Prisant, M.G., Richardson, J.S., and Richardson, D.C. (2003). Structure validation by Calpha geometry: phi,psi and Cbeta deviation. Proteins *50*, 437–450.

Masai, H., Taniyama, C., Ogino, K., Matsui, E., Kakusho, N., Matsumoto, S., Kim, J.M., Ishii, A., Tanaka, T., Kobayashi, T., et al. (2006). Phosphorylation of MCM4 by Cdc7 kinase facilitates its interaction with Cdc45 on the chromatin. J. Biol. Chem. *281*, 39249–39261.

McCoy, A.J., Grosse-Kunstleve, R.W., Adams, P.D., Winn, M.D., Storoni, L.C., and Read, R.J. (2007). Phaser crystallographic software. J. Appl. Cryst. *40*, 658–674.

Moyer, S.E., Lewis, P.W., and Botchan, M.R. (2006). Isolation of the Cdc45/Mcm2-7/GINS (CMG) complex, a candidate for the eukaryotic DNA replication fork helicase. Proc. Natl. Acad. Sci. USA *103*, 10236–10241.

Muramatsu, S., Hirai, K., Tak, Y.S., Kamimura, Y., and Araki, H. (2010). CDK-dependent complex formation between replication proteins Dpb11, Sld2, Pol (epsilon, and GINS in budding yeast. Genes Dev. *24*, 602–612.

Murshudov, G.N., Vagin, A.A., and Dodson, E.J. (1997). Refinement of macromolecular structures by the maximum-likelihood method. Acta Crystallogr. D Biol. Crystallogr. *53*, 240–255.

Nakajima, R., and Masukata, H. (2002). SpSld3 is required for loading and maintenance of SpCdc45 on chromatin in DNA replication in fission yeast. Mol. Biol. Cell *13*, 1462–1472.

Otwinowski, Z., and Minor, W. (1997). Processing of X-ray diffraction data collected in oscillation mode. Methods Enzymol. *276*, 307–326.

Sanchez-Pulido, L., and Ponting, C.P. (2011). Cdc45: the missing RecJ ortholog in eukaryotes? Bioinformatics *27*, 1885–1888.

Sanchez-Pulido, L., Diffley, J.F., and Ponting, C.P. (2010). Homology explains the functional similarities of Treslin/Ticrr and Sld3. Current biology: CB *20*, R509–510.

Sansam, C.L., Cruz, N.M., Danielian, P.S., Amsterdam, A., Lau, M.L., Hopkins, N., and Lees, J.A. (2010). A vertebrate gene, ticrr, is an essential checkpoint and replication regulator. Genes Dev. *24*, 183–194.

Sheu, Y.J., and Stillman, B. (2006). Cdc7-Dbf4 phosphorylates MCM proteins via a docking site-mediated mechanism to promote S phase progression. Mol. Cell *24*, 101–113.

Sheu, Y.J., and Stillman, B. (2010). The Dbf4-Cdc7 kinase promotes S phase by alleviating an inhibitory activity in Mcm4. Nature *463*, 113–117.

Szambowska, A., Tessmer, I., Kursula, P., Usskilat, C., Prus, P., Pospiech, H., and Grosse, F. (2014). DNA binding properties of human Cdc45 suggest a function as molecular wedge for DNA unwinding. Nucleic Acids Res. *42*, 2308–2319.

Tak, Y.S. (2004). Regulatory mechanism of the initiation of DNA replication by cyclin-dependent kinase. The Graduate University for Advanced Studies, Thesis dissertation.

Tanaka, S., Umemori, T., Hirai, K., Muramatsu, S., Kamimura, Y., and Araki, H. (2007). CDK-dependent phosphorylation of Sld2 and Sld3 initiates DNA replication in budding yeast. Nature *445*, 328–332.

Tanaka, S., Nakato, R., Katou, Y., Shirahige, K., and Araki, H. (2011a). Origin association of Sld3, Sld7, and Cdc45 proteins is a key step for determination of origin-firing timing. Current biology: CB *21*, 2055–2063.

Tanaka, T., Umemori, T., Endo, S., Muramatsu, S., Kanemaki, M., Kamimura, Y., Obuse, C., and Araki, H. (2011b). Sld7, an Sld3-associated protein required for efficient chromosomal DNA replication in budding yeast. EMBO J. *30*, 2019–2030.

Terwilliger, T.C. (2000). Maximum-likelihood density modification. Acta Crystallogr. D Biol. Crystallogr. *56*, 965–972.

Terwilliger, T.C. (2003). Automated main-chain model building by template matching and iterative fragment extension. Acta Crystallogr. D Biol. Crystallogr. *59*, 38–44.

Terwilliger, T.C., and Berendzen, J. (1999). Automated MAD and MIR structure solution. Acta Crystallogr. D Biol. Crystallogr. *55*, 849–861.

Yabuuchi, H., Yamada, Y., Uchida, T., Sunathvanichkul, T., Nakagawa, T., and Masukata, H. (2006). Ordered assembly of Sld3, GINS and Cdc45 is distinctly regulated by DDK and CDK for activation of replication origins. EMBO J. *25*, 4663–4674.

Yao, M., Zhou, Y., and Tanaka, I. (2006). LAFIRE: software for automating the refinement process of protein-structure analysis. Acta Crystallogr. D Biol. Crystallogr. *62*, 189–196.

Zegerman, P., and Diffley, J.F. (2007). Phosphorylation of Sld2 and Sld3 by cyclin-dependent kinases promotes DNA replication in budding yeast. Nature *445*, 281–285.